Laser and Particle Beams (2008), *26*, 207–212. Printed in the USA.
Copyright © 2008 Cambridge University Press 0263-0346/08 $20.00
doi:10.1017/S0263034608000232

Generation and confinement of high energy electrons generated by irradiation of ultra-intense short laser pulses onto cone targets

T. NAKAMURA,[1] K. MIMA,[1] H. SAKAGAMI,[2] T. JOHZAKI,[1] AND H. NAGATOMO[1]

[1]Institute of Laser Engineering, Osaka University, Suita, Japan
[2]Theory and Computer Simulation Center, National Institute for Fusion Science, Toki, Japan

(RECEIVED 21 January 2008; ACCEPTED 3 March 2008)

Abstract

Interactions of cone targets with different shapes with laser pulses are studied numerically. Two important parameters which characterize the laser-cone interaction in 2006 are introduced, which are cone angle and ratio of laser spot and cone tip. By changing these two parameters, energy coupling from laser to electrons is controlled. Some fraction of high energy electrons generated at side wall and cone tip are not freely propagating out from the target, but confined around the cone tip due to the disturbed electric field.

Keywords: Cone interaction; Fast ignition; High energy elecron generation; Laser

1. INTRODUCTION

Recent progress in laser technology opened new research fields in high energy density physics, such as X-ray generation with high brightness (Hartemann *et al.*, 2004), charged particle acceleration with high quality (Hatchett *et al.*, 2000; Katsouleas, 2004; Fuchs *et al.*, 2005; Flippo *et al.*, 2007; Karmakar & Pukhov, 2007; Koyama *et al.*, 2006, Lifschitz *et al.*, 2006; Nickles *et al.*, 2007; Yin *et al.*, 2006; Strangio *et al.*, 2007), fast ignition research in inertial fusion (Tabak *et al.*, 1994; Johzaki *et al.*, 2007; Sakagami *et al.*, 2006; Zvorykin *et al.*, 2007), and so on. In fast ignition scheme, cone targets are used to guide the heating laser pulse close to the core plasma which is surrounded by large-scale corona plasma, and to generate high energy charged particles which heat up the core. Advantages in using cone targets were confirmed in experiments, which show huge increase of neutron yield (Kodama *et al.*, 2002). But many physical issues are not clearly understood yet, which are now intensively studied experimentally and numerically (Stephens *et al.*, 2004; Chen *et al.*, 2005; Campbell *et al.*, 2005). One of the key issues among them is the generation of high energy particles from the cone target. It is shown in three-dimensional (3D) particle-in-cell (PIC) simulation that cone targets focus laser energy and high energy electrons at the cone tip which result in higher coupling efficiency from laser to electrons (Sentoku *et al.*, 1999). In this paper, we investigate the interaction between intense laser pulses and cone targets by using two-dimensional (2D) PIC simulation in order to study the cone geometry dependence on laser-cone interaction. We introduce two important parameters which characterize the laser-cone inetarction, and show the optimum value of them for fast ignition. To understand the dependence of laser-cone interaction on target geometry is crucial for designing the cone targets for fast ignition, and becoming basis for using them as the devices of generating high energy charged particles (Kodama *et al.*, 2004).

The paper is composed as follows. In Section 2, electron acceleration processes taking place in laser-cone interaction are studied and two parameters which characterize laser-cone interaction are introduced. In Section 3, the cone angle dependence on laser intensification and electron acceleration are studied. Electron confinement around cone tip is discussed. In Section 4, effect of another important parameter which is a ratio laser spot size and cone tip size is discussed. The conclusions are given in Section 5.

Address correspondence and reprint requests to: Tatsufumi Nakamura, Institute of Laser Engineering, Osaka University, Suita 565-0871, Japan. E-mail: nakamura@ile.osaka-u.ac.jp

https://doi.org/10.1017/S0263034608000232 Published online by Cambridge University Press

2. ELECTRON ACCELERATION PROCESSES IN LASER-CONE INTERACTION

First, we compare the electron characteristics generated from a cone target and a plane target which are irradiated by ultra-intense laser pulses. In Figure 1, electron spectra from the cone target and the plane target are plotted. Parameters and conditions of the cone target simulation are as follows. The target density is 100 times the critical density which is defined as $n_c = m\varepsilon_0\omega_0/e^2$ where m and e are the electron mass and the charge, ε_0 and ω are the dielectric constant in vacuum and the laser frequency, respectively. The preplasma exists inner side on the cone target which has exponential profile whose scale lengths are 1.0 μm and 0.27 μm at the cone tip and cone side wall, respectively. At the rear side of the cone target, overdense plasma which models the corona plasma is located whose density is $2n_c$. The initial electron temperature is 10 keV, and ions are kept immobile. The laser pulse irradiate the target from the left boundary whose intensity is 5.0×10^{19} W/cm^2 with 1.0 μm wavelength, which leads to the normalized vector potential which is defined by $a_0 = \sqrt{I\lambda_L^2/1.4 \times 10^{18}} = 6.0$, where I and λ_L are the laser intensity in units of W/cm^2 and the laser wavelength in unit of μm. The laser field is linearly polarized in the y-direction with a Gaussian profile whose spot size is 10.0 μm (full width at half maximum: FWHM). The laser pulse rises up in five laser cycles and sustains its peak intensity for 150 fs. A plane target is used for comparison, which is modeled to have the same conditions as the cone target, and is made by flattening the cone geometry into flat one, i.e., the target maximum density is $100n_c$ with preplasma of 1.0 μm scale length, and it is surrounded by $2n_c$ plasma at the rear side. The laser conditions are exactly the same as those used in the cone simulation.

In Figures 1a and 1b, time-integrated electron energy spectrums observed at 2 μm behind the targets are plotted. In plane target case, electron spectrum is fitted by Maxwell distribution with two temperatures. Lower temperature is 0.4 MeV for electrons with energy <2.0 MeV. Higher temperature is 2.5 MeV, which is well approximated by ponderomotive energy as $T_h = mc^2(\sqrt{1+a_0} - 1)$ (Wilks *et al.*, 1992). Electron spectrum from cone target shown in Figure 1b is fitted by Maxwell distribution with three temperatures. The lowest temperature is $T_{low} \sim 0.35$ MeV which is almost the same as in the plane case. But other two temperatures differ from the ponderomotive energy of incident laser pulse. The electrons whose energy is $2.0 \leq E \leq 5.0$ is fitted with $T_{mid} \sim 1.9$ MeV which is lower than the ponderomotive energy, and electrons with higher energy is fitted with $T_{high} \sim 5.0$ MeV, which is much higher than the ponderomotive energy of incident lasers. These two components account for electrons generated at cone wing and cone tip (Nakamura *et al.*, 2006, 2007). Since the laser irradiates the target obliquely, its intensity decreases on the surface, which results in electrons whose temperature is lower than initial ponderomotive energy. And at the cone tip, laser field is intensified due to multiple reflections, which results in electrons with temperature higher than ponderomotive energy.

These results indicate that there are two dominant acceleration processes taking place in laser-cone interaction; acceleration at wing and tip. The acceleration at cone wing depends on laser intensity and more importantly, cone angle, since the interaction strongly depends on incident angle for oblique irradiation. The acceleration at the cone tip depends on cone-focused laser fields, which is characterized by the ratio of laser spot size and cone tip as well as cone angle. Therefore two parameters which are cone angle and laser spot/cone tip ratio are characterizing the laser-cone interaction. In the following sections, we show how these parameters characterize the interaction and optimize them for the fast ignition.

3. ELECTRON CONFINMENT AROUND THE CONE TIP

The laser-cone interaction depends on the cone angle because the irradiation angle of laser field at cone sidewall and the

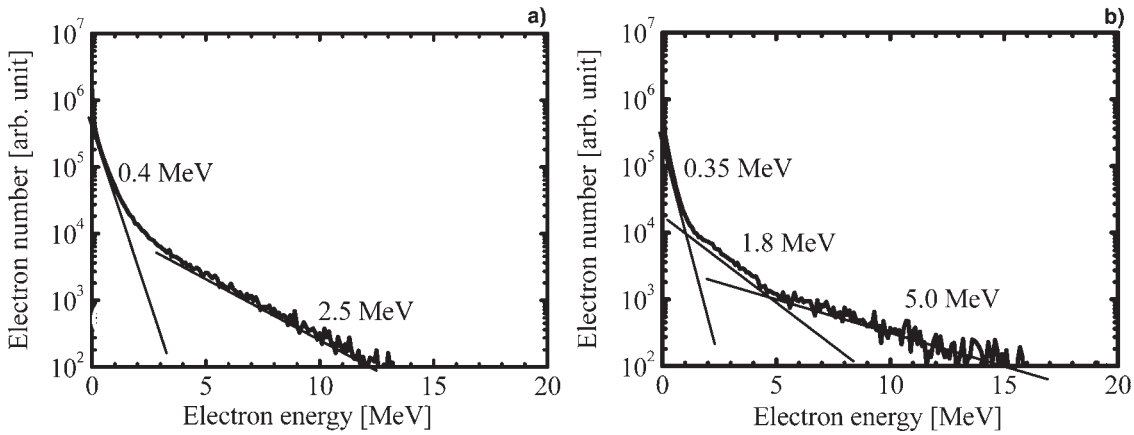

Fig. 1. Comparison of electron energy spectrums generated from (**a**) cone target and (**b**) plane target. Spectra are observed at target rear side, which are irradiated by intense laser pulses of 1.5×10^{19} W/cm^2 and 150 fs.

https://doi.org/10.1017/S0263034608000232 Published online by Cambridge University Press

propagation path of laser light inside cone change. The laser light irradiates cone sidewall with relatively large angle, e.g., 75° for 30° cone target. The energy absorption rate drastically changes around irradiation angle of 75° (Ruhl & Cairns, 1997), which is the case of laser-cone interaction. In addiction to the irradiation angle, the laser light propagation inside the cone target changes due to the cone angle.

A sample ray of laser light propagating in 30° cone target is drawn in Figure 2, where the specular reflection at wall is assumed. The laser light reflects four times before the light propagates backward, and the light located within 2R at the cone entrance is focused down to 0.53R spot diameter, indicating that laser light is intensified at cone tip about four times. The reflection angle is bigger for cone targets with larger cone angle, which results in less reflection time for larger angle cone targets, such as three times reflection in 45° cone and two times reflection in 60° cone. This affects the energy absorption rate.

In Table 1, the energy absorption rate evaluated by PIC simulation is shown for different cone angle. The simulation conditions are following. The laser intensity is 1.0×10^{20} W/cm^2 with duration of 150 fs whose spot size is 10 μm. The target density is $100n_c$, and diameter is 30 μm at cone entrance and 3 μm at the cone tip. As the cone angle becomes larger, the reflection time decreases to reduce absorption rate. When the high energy coupling from laser to electron is desired such as the fast ignition, cone targets with smaller angle are beneficial. Since the absorption rate sharply drops as the irradiation angle goes over 75°, 30° is small enough for achieving the high absorption rate.

In Table 1, along with the absorption rate, the ratio of the energy which is stored inside cone at 300 fs after terminating the laser pulse to the input laser energy is written. Even 300 fs later the termination, roughly half of the absorbed energy is still left inside the cone target. The temporal evolution of energy stored inside target for 30° cone is shown in Figure 3. These results show that the energy absorbed by the cone target is not released smoothly from the target. For high energy electrons flow out, the return current to sustain current-neutrality is necessary, which is achieved by the compensation of the bulk electrons. The electric field is induced to accelerate and heat up the bulk electrons for the compensation.

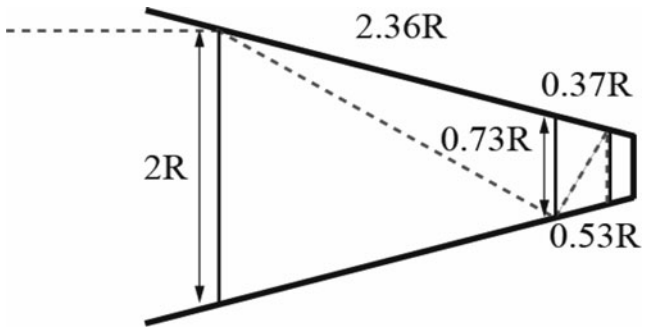

Fig. 2. A sample ray of light propagation inside 30° cone target. The rays located in 2R at cone entrance are focused to the diameter of 0.53R.

Table 1. *Energy flux ratio of electrons propagating out from cone to input laser in left column and absorption rate in right column. The ratio of stored energy to laser energy is also written in side the bracket*

	Flux ratio	Absorption rate (stored in cone)
30°	18.0	55 (25)
40°	16.9	49 (26)
60°	17.5	41 (19)

The distributions of electron kinetic energy and electromagnetic field energy at 150 fs after terminating the laser pulse are shown in Figure 4. It is clearly shown that high energy electrons are confined around the cone tip and prevented from flowing out. Electric and magnetic field energy is also localized around the cone tip. The electric field is disturbed and turbulent, which confine electrons at the tip. This phenomenon depends on target conductivity, therefore on target material, temperature, density, and so on. In the above simulation, the current density flowing in the forward direction toward the cone tip reaches up to $25 \times (-en_c c)$. When there exist abundant free and relatively high energy bulk electrons, which ensures current neutrality, this disturbed electric field is not induced.

This confinement is not negligible in fast ignition since the moderate energy electrons (~ 1 MeV) are kept releasing from the cone target toward core plasma for relatively long time. This long time effect is studied in integrated simulation of 1D-PIC and 2D Fokker-Planck code and shown to be important in the core heating (Sakagami *et al.*, 2006).

4. DEPENDENCE OF RATIO BETWEEN LASER SPOT AND CONE TIP ON LASER-CONE INTERACTION

In addition to the cone angle, the ratio between the laser spot and cone tip determines how much the laser field is

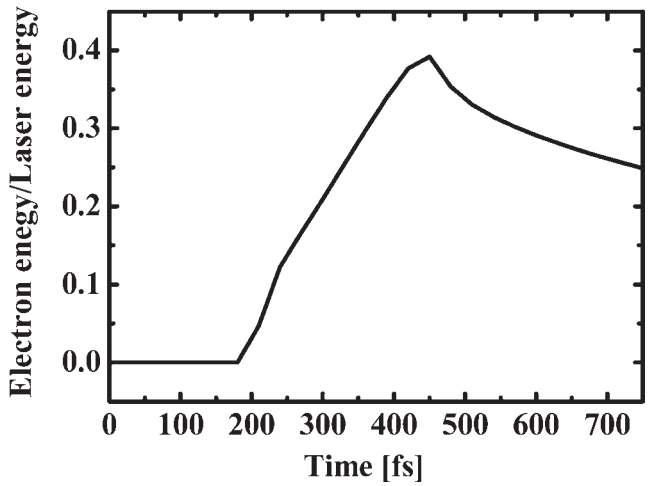

Fig. 3. Temporal evolution of electron energy inside the cone target. The energy is gradually released from the cone target after the laser irradiation.

https://doi.org/10.1017/S0263034608000232 Published online by Cambridge University Press

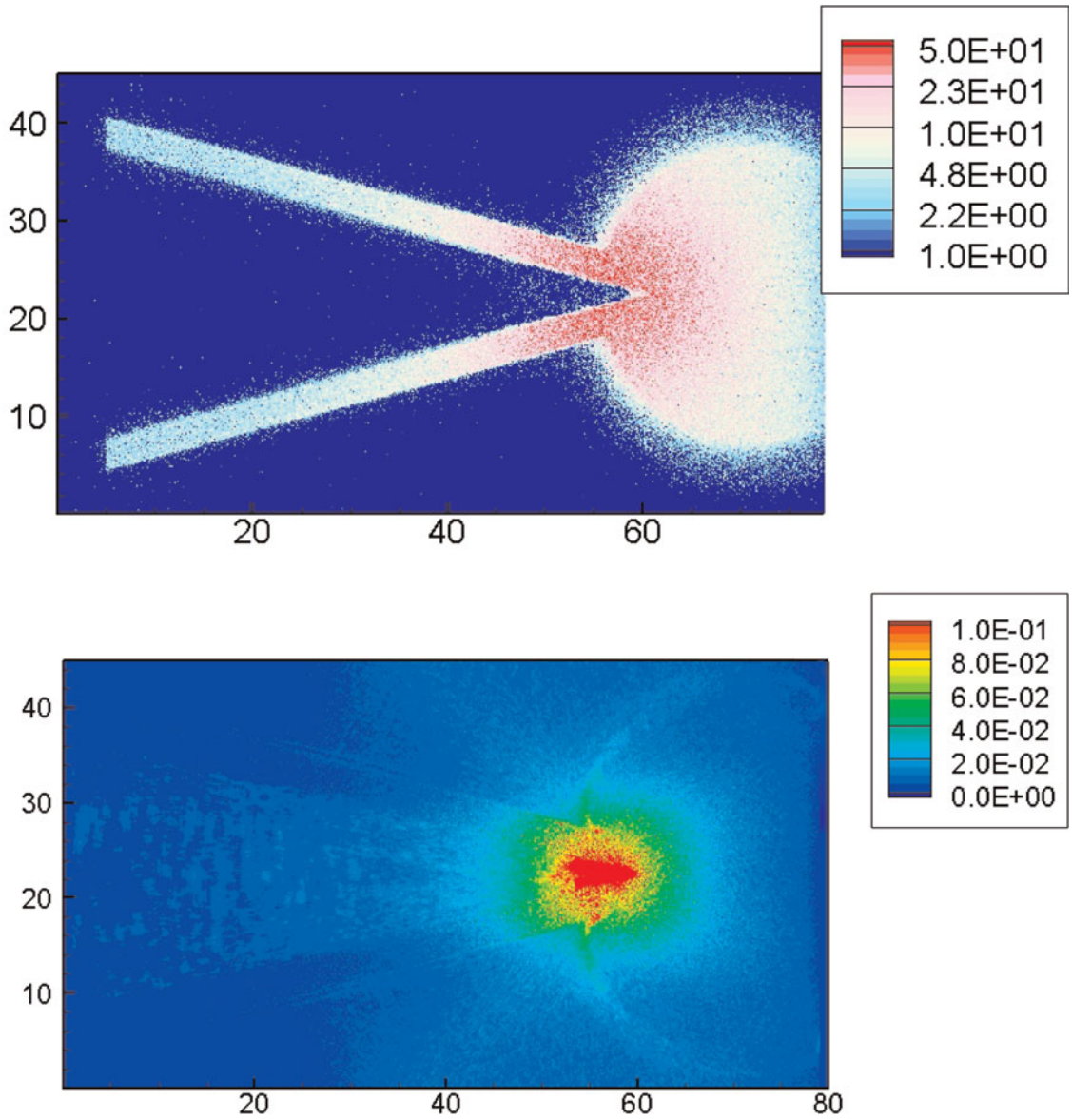

Fig. 4. (Color online) (top) Electron kinetic energy density distribution which is normalized by $n_c mc^2$. (bottom) Electric and magnetic field energy $(E^2 + B^2)/2$ which is normalized by $n_c mc^2$.

intensified at the cone tip by the cone guiding. The cone targets with different cone tip size by keeping the cone angle and the entrance diameter are compared. The diameter at entrance is 30 μm and diameter at tip is varied as 0, 3, 5, and 10 μm. The cone angle is 30° and the target density is $100n_c$. The electron temperature is 1 keV with immobile ions. The laser spot size is 10 μm in diameter and intensity is 1.0×10^{21} W/cm^2 with duration of 150 fs. In Table 2, the energy absorption rate and energy flux through the cone tip within 3 μm diameter are summarized. As the tip size becomes smaller, the interaction region at cone wing increases and the laser field is intensified more at the cone tip, which results in higher coupling. But the energy flux passing through the tip is maximum for 3 μm case, since the high energy electrons highly concentrated at the cone tip, which leads to diverging of the beam due to the space

Table 2. *Energy flux ratio of electrons propagating out from cone to input laser (left) and absorption rate (right) for cone targets with different cone tip size. The laser focus spot and diameter of cone entrance are same for all simulations*

	Flux ratio	Absorption rate [%]
0 mm	18.0	55
3 mm	24.2	52
5 mm	20.0	48
10 mm	18.3	43

https://doi.org/10.1017/S0263034608000232 Published online by Cambridge University Press

charge. Numerical simulations also show that the electron energy flux at rear side of the cone target is localized within the diameter comparable to the tip size. As a result, the tip diameter is chosen to be small enough to focus laser light on the tip and to increase absorption rate, and large enough to prevent the excess concentration of high energy electrons. For 30° cone targets, the spot size of about one-fourth of laser spot diameter is maximizing the wall interaction and focus all the laser beam to the tip. For a smaller tip, the laser light irradiating at the cone entrance outside the circle whose diameter is about four times the tip diameter does not reach to the tip. For a larger tip, laser intensification is smaller and wall interaction length is also shorter, which results in smaller absorption. In reality, the reflection at wall is not specular and laser profile at the tip is modulated by pre-plasmas. So the number one-fourth is not the strict number, but gives an insight in designing the cone target.

CONCLUSIONS

The laser-cone interaction is studied by 2D PIC simulations. Two important parameters which characterize the laser-cone interaction are introduced, which are cone angle and ratio of laser spot and tip diamter. These paramters control the laser propagation inside the target, laser intensification at the tip, and wall interaction. For the angle, 30° cone target is suitable for fast ignition since the high energy absorption and high energy flux. For the ratio of laser spot and tip diameter, about one-fourth of tip size is maximizing the lsaer fucusing effect and wall interaction. The confinement of high energy electrons at cone tip is observed, which is due to the disturbed electric field at the cone tip. The electric field is generated in order to satisfy the current neutrality. Therefore, the phenomena depends on the target conditions, such as material, density, temperature and so on. Further study of this effect on electron transport in fast ignition is considered to be necessary.

REFERENCES

Campbell, R.B., Kodama, R., Melhorn, T.A., Tanaka, K.A. Welch, D.R. (2005). Simulation of heating-compressed fast-ignition cores by petawatt laser-generated electrons. *Phys. Rev. Lett* **94**, 055001.

Chen, Z.L., Kodama, R., Nakatsutsumi, M., Nakamura, H., Tampo, M., Tanaka, K.A., Toyama, Y., Tsutsumi, T. & Yabuuchi, T. (2005). Enhancement of energetic electrons and photons by cone guiding of laser light. *Phys. Rev. E* **71**, 036403–036407.

Flippo, K., Hegelich, B.M., Albright, B.J., Yin, L., Gautier, D.C., Letzring, S., Schollmeier, M., Schreiber, J., Schulze, R. & Fernandez, J.C. (2007). Laser-driven ion accelerators: Spectral control, monoenergetic ions and new acceleration mechanisms. *Laser Part. Beams* **25**, 3–8.

Fuchs, J., Sentoku, Y., Karsch, S., Cobble, J., Audebert, P., Kemp, A., Nikroo, A., Antici, P., Brambrink, E., Blazevic, A., Campbell, E.M., Fernandez, J.C., Gauthier, J.C., Geissel, M., Hegelich, M., Pepen, H., Poescu, H., Renard-Legalloudec, N., Roth, M., Schreiber, J., Stephens, R. & Cowan, T.E. (2005). Comparison of laser ion acceleration from the front and rear surfaces of thin foils. *Phys. Rev. Lett*. **94**, 045004.

Hartemann, F.V., Tremaine, A.M., Anderson, S.G., Barty, C.P.J., Betts, S.M., Booth, R., Brown, W.J., Crane, J.K., Cross, R.R., Gibson, D.J., Fittinghoff, D.N., Kuba, J., Le Sage, G.P., Slaughter, D.R., Wootton, A.J., Hartouni, E.P., Springer, P.T., Rosenzweig, J.B. & Kerman, A.K. (2004). Characterization of a bright, tunable, ultrafast Compton scattering X-ray source. *Laser Part. Beams* **22**, 221–244.

Hatchett, S.P., Brown, C.G., Cowan, T.E., Henry, E.A., Johnson, J.S., Key, M.H., Koch, J.A., Langdon, A.B., Lasinski, B.F., Lee, R.W., Mackinnon, A.J., Pennington, D.M., Perry, M.D., Phillipps, T.W., Roth, M., Sangste, T.C., Singh, M.S., Snavely, R.A., Stoyer, M.A., Wilks, S.C. & Yasuike, K. (2000). Electron, photon, and ion beams from relativistic interaction of Petawatt laser pulses with solid targets. *Phys. Plasmas* **7**, 2076–2082.

Johzaki, T., Sakagami, H., Nagatomo, H. & Mima, K. (2007). Holistic simulation for FIREX project with FI3. *Laser Part. Beams* **25**, 621–629.

Johzaki, T., Nagatomo, H., Sakagami, H., Nakamura, T., Mima, K., Nakao, Y. & Yokota, T. (2006). Core heating analysis of fast ignition targets by integrated simulations. *J. Phys. IV France* **133**, 385

Karmakar, A. & Pukhov, A. (2007). Collimated attosecond GeV electron bunches from ionization of high-Z material by radially polarized ultra-relativistic laser pulses. *Laser Part. Beam* **25**, 371–377.

Katsouleas, T. (2004). Electrons hang ten on laser wake. *Nature* **431**, 515–516.

Kodama, R., Sentoku, Y., Chen, Z.L., Kumar, G.R., Hatchett, S.P., Toyama, Y., Cowan, T.E., Freeman, R.R., Fuchs, J., Izawa, Y., Key, M.H., Kitagawa, Y., Kondo, K., Matsuoka, T., Nakamura, H., Nakatsutsumi, M., Norreys, P.A., Norimatsu, T., Snavely, R.A., Stephens, R.B., Tampo, M., Tanaka, K.A. & Yabuuchi, T. (2004). Plasma devices to guide and collimate a high density of MeV electrons. *Nature* **432**, 1005–1008.

Kodama, R., Shiraga, H., Shigemori, K., Toyama, Y., Fujioka, H., Azechi, H., Fujita, H., Habara, H., Hall, T., Izawa, Y., Jitsuno, T., Kitagawa, Y., Krushelnick, K.M., Lancaster, K.L., Mima, K., Nagai, K., Nishimura, H., Norimatsu, T., Norreys, P.A., Sakabe, S., Tanaka, K.A., Youssef, A., Zepf, M. & Yamanaka, T. (2002). Fast heating scalable to laser fusion ignition. *Nature* **418**, 933–934.

Koyama, K., Adachi, M., Miura, E., Kato, S., Masuda, S., Watanabe, T., Ogata, A. & Tanimoto, M. (2006). Monoenergetic electron beam generation from a laser-plasma accelerator. *Laser Part. Beams* **24**, 95–100.

Lifschitz, A.F., Faure, J., Glinec, Y., Malka, V. & Mora, P. (2006). Proposed scheme for compact GeV laser plasma accelerator. *Laser Part. Beams* **24**, 255–259.

Nakamura, T., Sakagami, H., Johzaki, T., Nagatomo, H. & Mima, K. (2006). Generation and transport of fast electrons inside cone targets irradiated by intense laser pulses. *Laser Part. Beams* **24**, 5–8.

Nakamura, T., Sakagami, H., Johzaki, T., Nagatomo, H., Mima, K & Koga, J. (2007). High energy electron generation by laser-cone interaction. *J. Plasma Fusion Res* **2**, 0018.

Nickles, P.V., Ter-Avetisyan, S., Schnuerer, M., Sokollik, T., Sandner, W., Schreiber, J., Hilscher, D., Jahnke, U., Andreev, A. & Tikhonchuk, V. (2007). Review of ultrafast ion

https://doi.org/10.1017/S0263034608000232 Published online by Cambridge University Press

acceleration experiments in laser plasma at Max Born Institute. *Laser Part. Beams* **25**, 347–363.

Ruhl, H. & Cairns, R.A. (1997). Reduced fractional absorption and second harmonic emission in laser-produced plasmas. *Phys. Plasmas* **4**, 2246.

Sakagami, H., Johzaki, T., Nagatomo, H. & Mima, K. (2006). Fast ignition integrated interconnecting code project for cone-guided targets. *Laser Part. Beams* **24**, 191–198.

Sentoku, Y., Ruhl, H., Mima, K., Kodama, R., Tanaka, K.A. & Kishimoto, Y. (1999). Plasma jet formation and magnetic field generation in the intense laser plasma under oblique incidence. *Phys. Plasmas* **6**, 2855–2861.

Stephens, R.B., Snavely, R.A., Aglintskiy, Y., Amiranoff, F., Andersen, C., Batani, D., Baton, S.D., Cowan, T., Freeman, R.R., Hall, T., Hachett, S.P., Hill, J.M., Key, M.H., King, J.A., Koch, J.A., Koenig, M., Mackinnon, A.J., Lancaster, K.L., Martinolli, E., Norreys, P., Perelli-Cippo, E., Rabec-Legloahec, M., Rousseaux, C., Santos, J.J. & Scianitti, F. (2004). Kα fluorescence measurement of relativistic electron transport in the context of fast ignition. *Phys. Rev. E* **69** 066414–066420.

Strangio, C., Caruso, A., Neely, D., Andreoli, P.L., Anzalone, R., Clarke, R., Cristofari, G., Del Prete, E., Di Giorgio, G., Murphy, C., Ricci, C., Stevens, R. & Tolley, M. (2007). Production of multi-MeV per nucleon ions in the controlled amount of matter mode (CAM) by using causally isolated targets. *Laser Part. Beams* **25**, 85–91.

Tabak, M., Hammer, J., Glinsky, J., Kruer, W.L., Wils, S.C., Woodworth, J., Campbell, M., Perry, M. & Mason, R.J. (1994). Ignition and gain with ultrapowerful lasers. *Phys. Plasmas* **1**, 1626–1634.

Wilks, S.C., Kruer, W.L., Tabak, M. & Langdon, A.B. (1992). Absorption of ultra-intense laser pulses. *Phys. Rev. Lett* **69**, 1383–1386.

Yin, L., Albright, B.J., Hegelich, B.M. & Fernandez, J.C. (2006). GeV laser ion acceleration from ultrathin targets: The laser break-out afterburner. *Laser Part. Beams* **24**, 291–298.

Zvorykin, V.D., Didenko, D.V., Ionin, A.A., Kholin, I.V., Konyashchenko, A.V., Krokhin, O.N., Levchenko, A.O., Mavritskii, A.O., Mesyats, G.A., Molchanov, A.G., Rogulev, M.A., Seleznev, L.V., Sinitsyn, D.V., Tenyakov, S.Y., Ustinovskii, N.N. & Zayarnyi, D.A. (2007). GARPUN-MTW: A hybrid Ti: Sapphire/KrF laser facility for simultaneous amplification of subpicosecond/nanosecond pulses relevant to fast-ignition ICF concept. *Laser Part. Beams* **25**, 435–451.

https://doi.org/10.1017/S0263034608000232 Published online by Cambridge University Press